FSI-08-TN79

THE ELASTIC MEMBRANE AND WALL MODEL IN *FLOW-3D*

Gengsheng Wei
Flow Science, Inc.
July 2008

---

1. Introduction

An elastic membrane and wall model has been developed to provide a limited Fluid-Structure Interaction (FSI) capability in ***FLOW-3D***. In the model, deformation of an elastic membrane or an elastic wall impacts the adjacent fluid flow, while fluid pressure, in turn, affects the deformation. These interactions are described in the code in a fully coupled fashion.

The main assumption of the model is that the deformations are small, i.e., the deflections are much smaller than the size of the deforming object (for elastic membranes) or the characteristic lengths of fluid flow and wall thickness (for elastic walls), allowing for a few useful simplifications. The geometries of membranes and elastic walls are assumed to be time-invariant, while the effects of their deformation on fluid flow are described with volume sources and sinks distributed along the fixed fluid-structure interface. With the further assumption that the pressure force is uniformly distributed on the membrane surface, analytical solutions rather than structural analysis algorithms are used to determine the membrane deformation.

There are many potential applications for the model in microfluidic systems, e.g., chemical analysis systems, medical microdosage systems and inkjet devices. The model can be used to simulate flow in piezoelectric valveless pumps which convert membrane vibrations into a pumping action. The model can also be used to simulate droplet formation for piezoelectric inkjet printheads where a membrane or an elastic tube deforms under the force of a piezoelectric actuator to produce a droplet of ink.

2. Elastic Membrane Deformation

An elastic membrane is a rectangular or circular thin plate undergoing a small elastic deformation under external forces. Its thickness and material properties are assumed uniform. Its edge can be either simply supported or clamped. A simply supported edge is one having both zero deflection and zero net force moment. At a clamped edge, however, both deflection and its first order derivatives are zero, but the force moment is usually non-zero. In any case, the model requires that a membrane has only *one* of those two conditions present at *all* its edges. There is no restriction on the location of a membrane in the computational domain, but the membrane's deforming surface must be perpendicular to the *x*, *y*, or *z* axis.

The model considers two external forces acting on a membrane: the hydraulic pressure force and the actuator force. The hydraulic force is obtained by the integration of pressure over both sides of the membrane and is then converted into a uniformly distributed force over the whole membrane. Users can prescribe the actuator force either as a sinusoidal or a piecewise linear function of time. In the model, the actuator is always assumed to be positioned coaxially on the membrane, and the contact area has the same shape (but not necessarily the same size) as the membrane. Because the actuator itself usually has much lower rigidity than the membrane, it is further assumed that the actuator force is uniformly distributed over the contact area. If a zero actuator contact area is given, then the actuator force is treated as a concentrated force at the membrane's center.

For a better computational efficiency, the analytical solutions rather than structural analysis algorithms are used to calculate the membrane's deformation in response to the transient pressure and actuator forces. The inertia of the membrane is neglected, therefore, at any point in time the membrane is assumed to be at an equilibrium state defined by the balance of the hydraulic force, actuator force and the membrane's rigidity. The analytical solutions are obtained by solving the equilibrium equation for a thin plate with small deformation,

$$\nabla^2\nabla^2 w = \frac{f}{D} \quad , \tag{1}$$

where w is the deflection, f is the net external force per unit area on the membrane, and D is flexural rigidity,

$$D = \frac{Eh^3}{12(1-\nu^2)} \ , \tag{2}$$

where E is Young's modulus, ν is Poisson's ratio, and h is the membrane's thickness.

Consider a rectangular membrane with its surface perpendicular to the z axis. In a Cartesian coordinate system, Equation (1) is written as

$$\frac{\partial^4 w}{\partial x^4} + 2\frac{\partial^4 w}{\partial x^2 \partial y^2} + \frac{\partial^4 w}{\partial y^4} = \frac{f}{D} \ . \tag{3}$$

For convenience, let the origin be placed at the membrane's center, and a and b represent the membrane's lengths in x and y directions, respectively. The boundary conditions for the membrane with the simply supported edges are

$$w = 0 \quad \text{and} \quad \frac{\partial^2 w}{\partial x^2} = 0 \qquad \text{for } x = \pm\frac{a}{2},$$
$$w = 0 \quad \text{and} \quad \frac{\partial^2 w}{\partial y^2} = 0 \qquad \text{for } y = \pm\frac{b}{2}.$$

If the membrane has clamped edges, the boundary conditions are

$$w = 0 \quad \text{and} \quad \frac{\partial w}{\partial x} = 0 \qquad \text{for } x = \pm\frac{a}{2},$$
$$w = 0 \quad \text{and} \quad \frac{\partial w}{\partial y} = 0 \qquad \text{for } y = \pm\frac{b}{2},$$

For a circular membrane, it is convenient to write Equation (1) in a cylindrical coordinate system with its origin located at the membrane's center and the *z* axis directed along the membrane's symmetry axis,

$$\frac{1}{r}\frac{d}{dr}\left\{r\frac{d}{dr}\left[\frac{1}{r}\frac{d}{dr}\left(r\frac{dw}{dr}\right)\right]\right\} = \frac{f}{D} \quad . \tag{4}$$

With *a* denoting the membrane's radius, the boundary condition for the simply supported edge is

$$w = 0 \quad \text{and} \quad \frac{\partial^2 w}{\partial r^2} = 0, \qquad \text{for } r = a.$$

For the clamped edge, the boundary condition is

$$w = 0 \quad \text{and} \quad \frac{\partial w}{\partial r} = 0, \qquad \text{for } r = a.$$

All the analytical solutions for the membrane's deflection used in the model satisfy the above equations. Some of these solutions are found in Timoshenko and Woinowsky-Krieger (1959), while the others are derived from the existing solutions using the supposition method. Please refer to Appendix A for the full solutions.

To account for the effects of the membrane motion on fluid flow, the continuity equation for fluid is modified with a volume source (or sink) term *S* added to its right-hand side,

$$\frac{V_f}{\rho}\frac{\partial \rho}{\partial t} + \frac{1}{\rho}\nabla\cdot(\rho\vec{u}A_f) = S \tag{5}$$

where ρ is the fluid density, *u* is the fluid velocity and A_f and V_f are the area and volume fractions, or porosity factors (***FLOW-3D*** manual). In a mesh cell,

$$S = \frac{S_{mb}}{V_{cell}}\vec{V}_{mb}\cdot\vec{n} \tag{6}$$

where V_{cell} is the total volume of the mesh cell, and S_{mb} , $\vec{n}$ and $\vec{V}_{mb}$ are the surface area, the unit outward normal and the velocity of the membrane surface in the mesh cell, respectively.

The transport equation for the VOF function is modified by adding the source term S given by Equation (6), multiplied by the fractional volume of fluid in a cell, F,

$$V_f \frac{\partial F}{\partial t} + \nabla \cdot (F\vec{u}A_f) = F \cdot S \tag{7}$$

Similar source terms are added to the energy and scalar transport equations. The transport equations for momentum and turbulence remain unchanged because they are used in their non-conservative forms. The non-conservative form of a transport equation is obtained by combining its conservative form with the continuity equation, in which case the source term cancels out.

3. Elastic Wall Deformation

An elastic wall in ***FLOW-3D*** is an object of an arbitrary shape. Its surface deformation is proportional to the pressure in the adjacent fluid, namely

$$w = -\frac{(p - p_{ref})}{K} \tag{8}$$

where w is local deflection of the wall surface in the direction of outer normal, p is the local pressure, p_{ref} is the reference pressure, and K is the stiffness coefficient per unit area. Such kind of elastic deformation occurs if Poisson's ratio for the wall material is zero, i.e., the normal stress causes no lateral strain. It is also a reasonable approximation when the normal deformation of the wall is very small, i.e. the lateral deformations will be negligible. With the lateral strain term neglected, Hooke's law is reduced to

$$\varepsilon = \frac{\sigma}{E} \tag{9}$$

where ε is the normal strain, σ is the normal stress, and E is Young's modulus. Note that in the model, the pressure is the only force affecting the deformation. No actuator force is considered. Every point on the surface of the wall deforms in the direction of the local surface normal.

K in Equation (8) is a user-prescribed parameter. To estimate its value, consider a plate with one side fixed and the other side under a normal force. Assume negligible Poisson's ratio and a uniform normal stress on its surface σ. At equilibrium, the normal stress must have the same value σ everywhere inside the plate. Let h and w represent the plate's thickness and deflection, respectively. The strain is then w/h, and Hooke's law in Equation (9) gives

$$w = \frac{\sigma}{E/h} \tag{10}$$

Equation (10) indicates that $K = \frac{E}{h}$. In general, K can be estimated as

$$K = \frac{E}{L} \tag{11}$$

where L is a characteristic depth of the elastic wall. It is noted that Equation (11) is only a rough estimate of K. Experimental measurement or a full structural analysis may be needed to obtain the accurate value of K.

Effects of the elastic wall motion on fluid flow are described by adding a fluid source (or sink) at the wall surface, similar to the way it is done in the membrane model, as described in Section 2.

4. Model Implementation

The model allows for multiple elastic membrane and elastic wall objects, each characterized by its shape, size, orientation and material properties. A membrane or an elastic wall is created as a regular geometry component. For a membrane, the dimensions and shape of the component do not have to be exactly the same as those of the actual membrane. For example, the extents of the component can be made larger than the size of the membrane to overlap the surrounding components to prevent potential leaks of fluid. The thickness of the component can also be larger than the actual membrane thickness so it can be resolved by the computational grid. It is most commonly encountered that fluid exists only at one side of the membrane. In such cases, the user only need be concerned that the location of the fluid side of the component matches the actual membrane location because the geometry differences between the component and the membrane do not affect the computational result if the component is defined larger than the membrane. The actual shape and dimensions of a membrane are defined separately using additional input variables. Conversely, the geometry of an elastic wall is defined by its geometry component.

The deflection coefficients are first calculated in each cell that contains a membrane or elastic wall surface. They are then used during simulation to calculate the deformations as functions of the applied total force in these cells. Deflection of a membrane is calculated with

$$w = k_p F_p + k_a F_a \tag{12}$$

where F_p and F_a are the total pressure force and the actuator force over the membrane. F_p is obtained by integrating the relative pressure $(p - p_{ref})$ over the whole open surface of the membrane. k_p and k_a in the equation are the deflection coefficients for pressure force and actuator force, respectively, and calculated using the equations in Appendix A. For the series expansions with infinite number of terms, only the first few terms of each expansion are considered. The number of these terms is determined through numerical tests for accuracy. In most cases, ten terms are sufficient to achieve a high accuracy. For an elastic wall, deflection in each solid boundary cell is calculated as

$$w = k_w(p - p_{ref}) \tag{13}$$

where k_w is the deflection coefficient for the elastic wall. Note the deflection coefficients k_p and k_a vary from cell to cell but are time-independent. k_w, however, is both location and time-independent.

The model uses an implicit approximation to describe the coupling of the deflections to the pressure in the fluid. At each time step, the solution for the deflections and pressure is obtained iteratively using under-relaxation. The default value of the relaxation factor OMEGA is 1.0 for the membrane model and 0.7 for the elastic wall model. If convergence difficulties arise, the relaxation factor is automatically reduced to help achieve convergence or a smaller relaxation factor can be specified during problem setup.

Due to the small deformation assumption, geometries of the membranes and elastic walls are fixed throughout the calculations, as defined by their initial setup. When computational results are displayed, deformations can be visualized by plotting the contours of the output variable *deflection*. Deflection of the membrane center versus time is available in the *General History Data* catalogue. The positive value of deflection is defined differently for a membrane and an elastic wall. The positive deflection of a membrane is in the positive direction of the coordinate axis which the membrane is perpendicular to. A positive wall deflection, however, corresponds to deformation in outward surface normal, i.e., into the fluid. The negative value of deflection is defined in the opposite direction correspondingly.

Restrictions and limitations exist in the model. In addition to assumption of small deflections, elastic membranes and walls cannot be porous or moving objects. If a moving object collides with a membrane or an elastic wall, the latter is treated as a non-moving rigid object, thus the impact affects only the motion of the moving object.

5. Validation and application

5.1. 3-D Piezo-acoustic inkjet device

Consider a simple piezo-acoustic inkjet device consisting of a long tube with a nozzle at one end and an ink reservoir at the other. There are two piezoelectric actuators inserted into the wall of the tube, as shown in Figure 1. The inner diameter and the length of the tube are 0.044 cm and 0.58 cm, respectively. The pipe's stiffness coefficient per unit area

is 10^{11} dyn/cm^3. The ink has a density of 1.06 g/cm^3 and a viscosity of 0.1 g/(cm·s). The reference and initial pressures are zero. Initially, the tube is full of ink at zero velocity. A voltage is then applied to each actuator to move the actuator away from the tube's centerline, causing an enlargement of the tube in its middle region. After a short time, the voltage is turned off returning the actuator to its original position. The actuators are modeled with the prescribed motion using the General Moving Object (GMO) model, with the radial velocity shown in Figure 2 as a function of time.

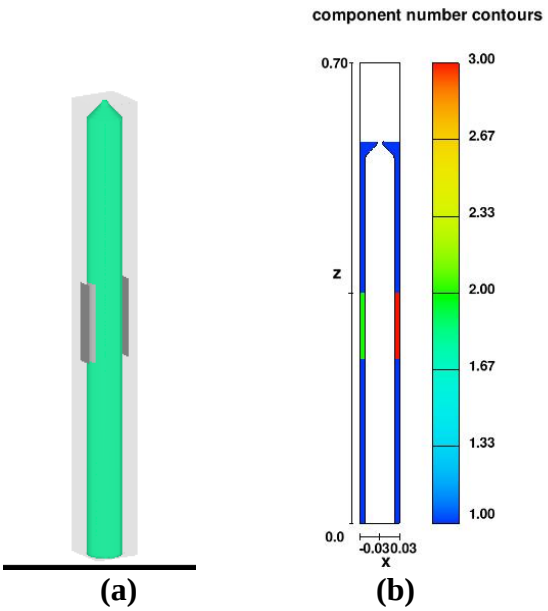

Figure 1. Geometry of the piezo-acoustic inkjet device: (a) 3-D geometry, (b) 2-D view in the central plane. Component 1: tube wall; components 2 and 3: actuators.

Figure 3 shows the calculated pressure distribution in the central plane at different times, illustrating the basic mechanism of the inkjet device. From time t=0.0 to 3.0×10^{-6} s, the tube is widened at its middle section due to the outward motion of the actuators. This initially forms a low pressure region which in turn generates two low pressure acoustic waves propagating toward the opposite ends of the tube. At about 1.25×10^{-5} s, both pressure waves reflect at their respective ends of the tube and move back towards the center in the form of high pressure waves. At about t=2.0×10^{-5} s, the two high pressure waves meet near the actuators. At the same time the actuators start moving back and reach their original positions at t=2.3×10^{-5} s, further raising the fluid pressure in this region and thus enhancing the intensity of the two waves. As one of them reaches the nozzle at t=3×10^{-5} s, the increased pressure in the wave pushes the ink out of the nozzle forming an ink droplet.

Figure 4 shows the time variations of the ink pressure and deflection of the tube wall at x=0.022 cm, y=0.0 cm and z=0.5 cm. The first trough in Figure 4 (a) is caused by the initial low pressure wave, and the subsequent two peaks are caused by the two high pressure waves as they pass that location. Figure 4 (a) and (b) clearly show the response

of deflection to the changes in local pressure. At a negative relative pressure, a positive deflection (in the wall's outer normal direction) occurs and the tube is narrowed. For a positive relative pressure the deflection is directed away from the axis, causing a widening of the cross-section. The pressure and the deflection curves satisfy Equation (13) exactly.

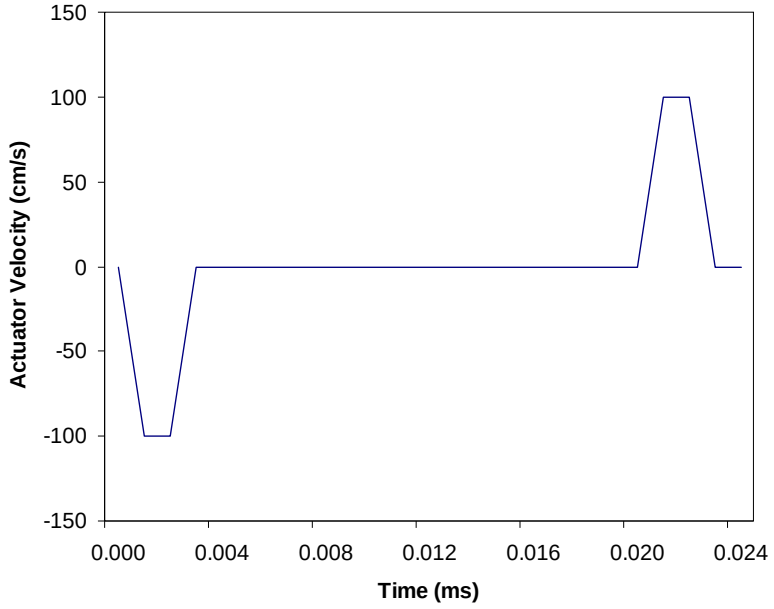

Figure 2. Actuator's prescribed radial velocity as a function of time.

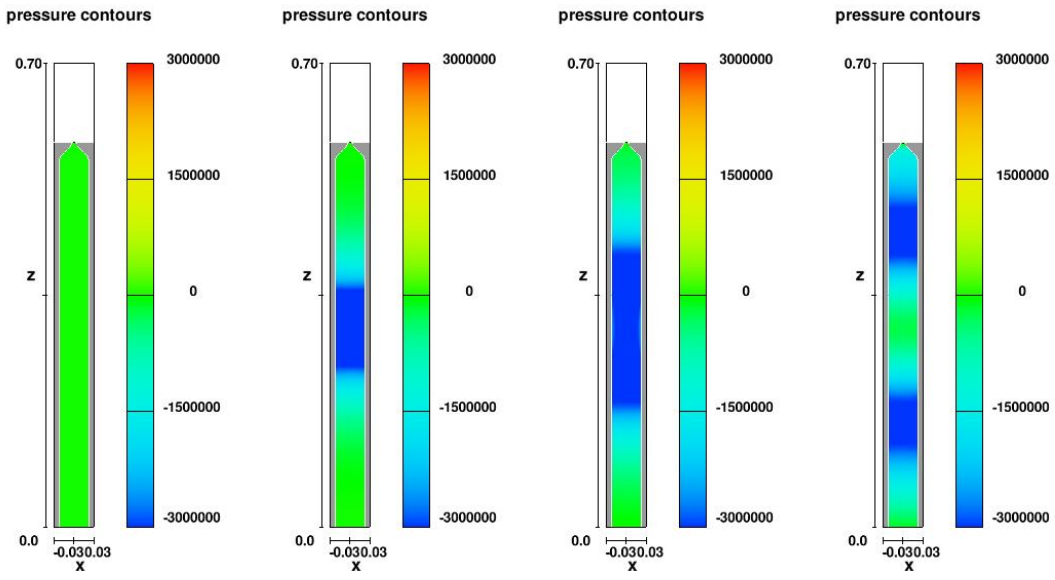

0.0 s 5×10^{-7} s 3×10^{-6} s 5.5×10^{-6} s

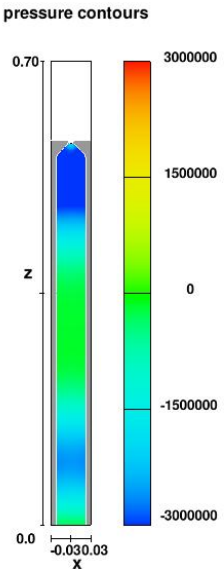

8×10^{-6} s

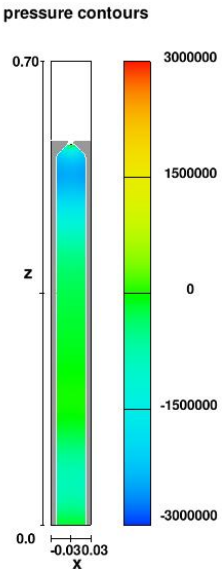

1×10^{-5} s

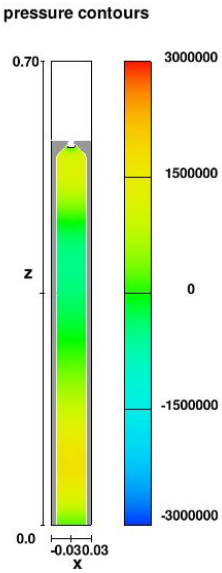

1.25×10^{-5} s

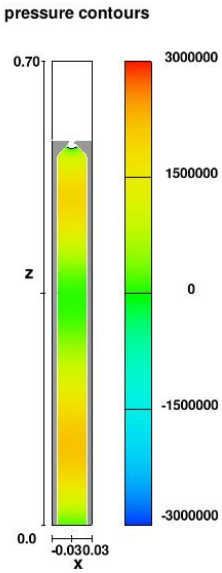

1.5×10^{-5} s

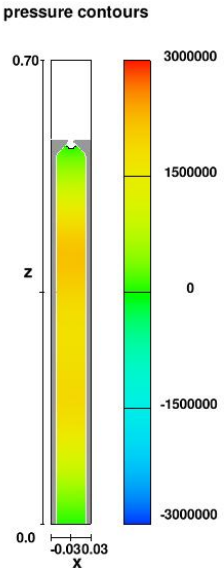

1.75×10^{-5} s

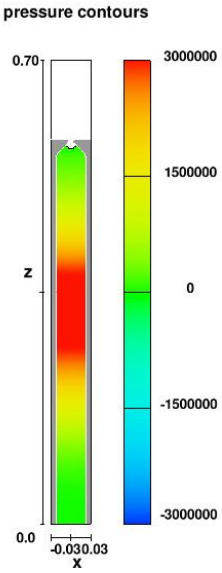

2×10^{-5} s

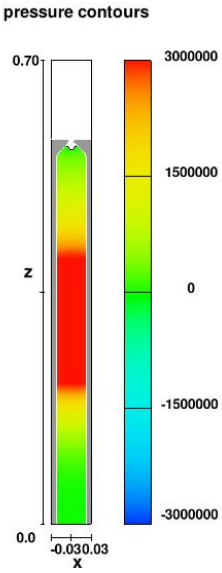

2.2×10^{-5} s

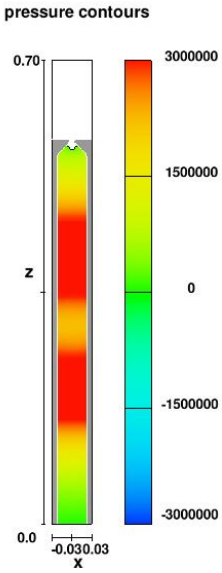

2.45×10^{-5} s

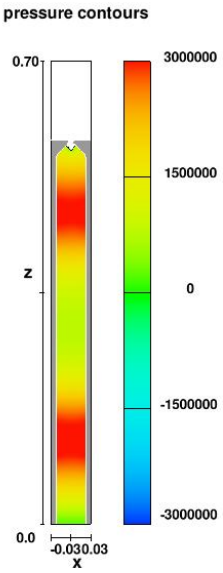

2.75×10^{-5} s

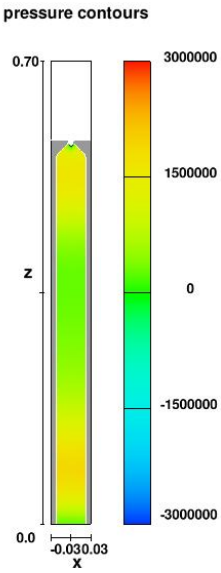

3×10^{-5} s

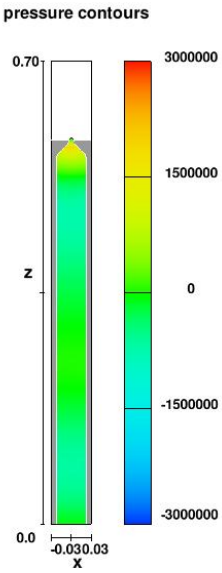

3.25×10^{-5} s

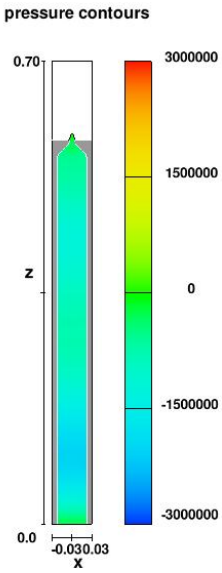

3.5×10^{-5} s

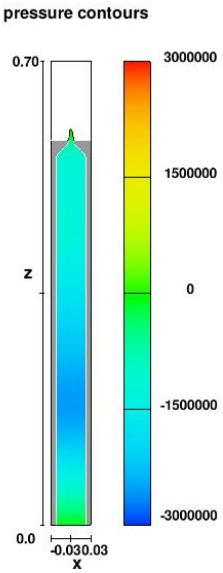

3.68×10^{-5} s

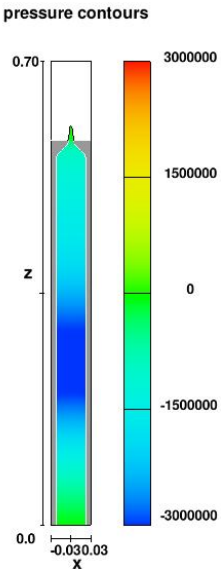

3.88×10^{-5} s

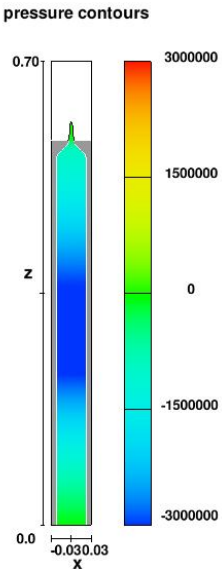

4.13×10^{-5} s

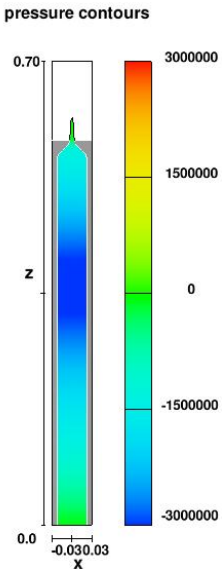

4.38×10^{-5} s

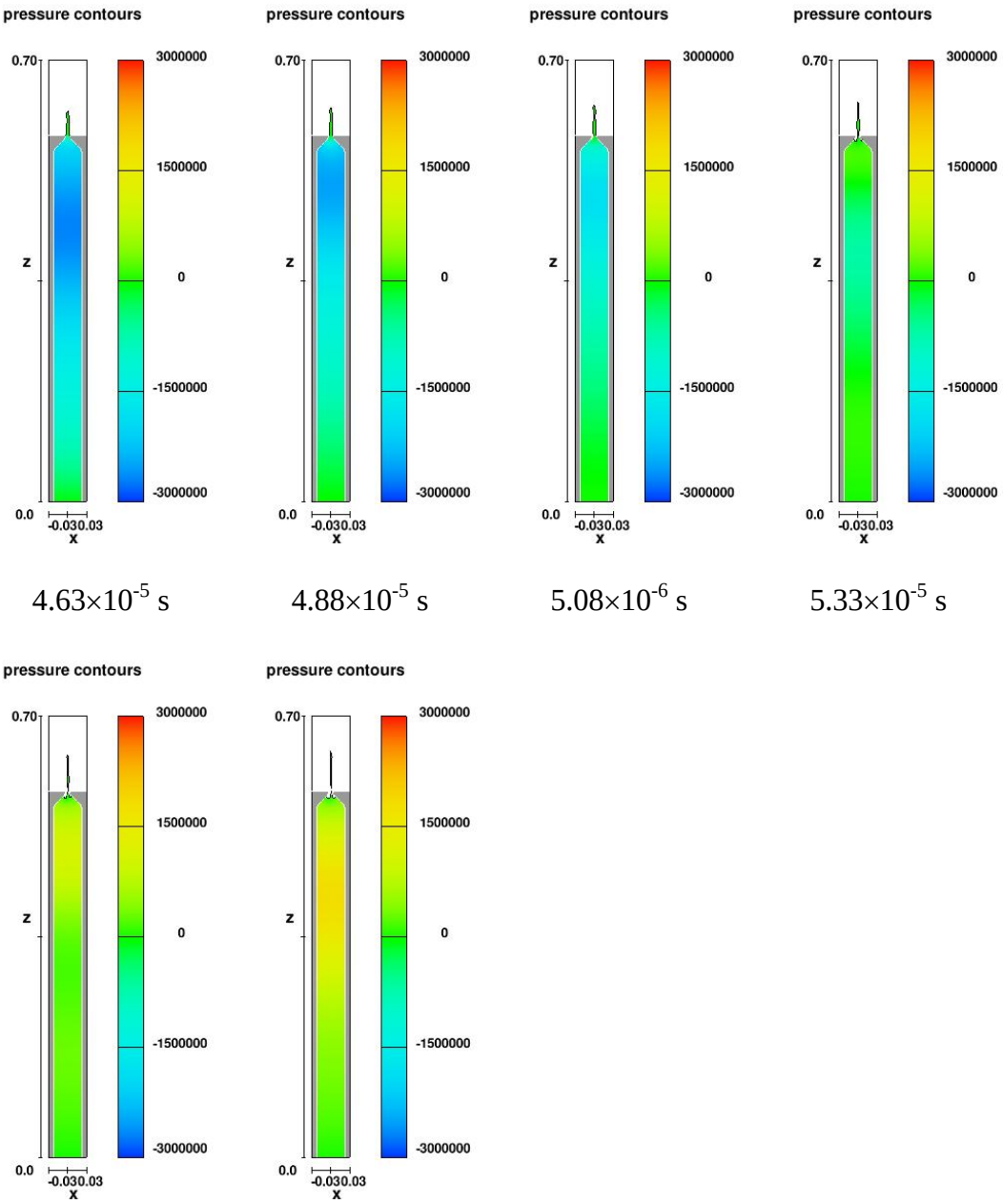

Figure 3. Pressure distribution (in dyne/cm^2) at the center plane of the piezo-acoustic inkjet device.

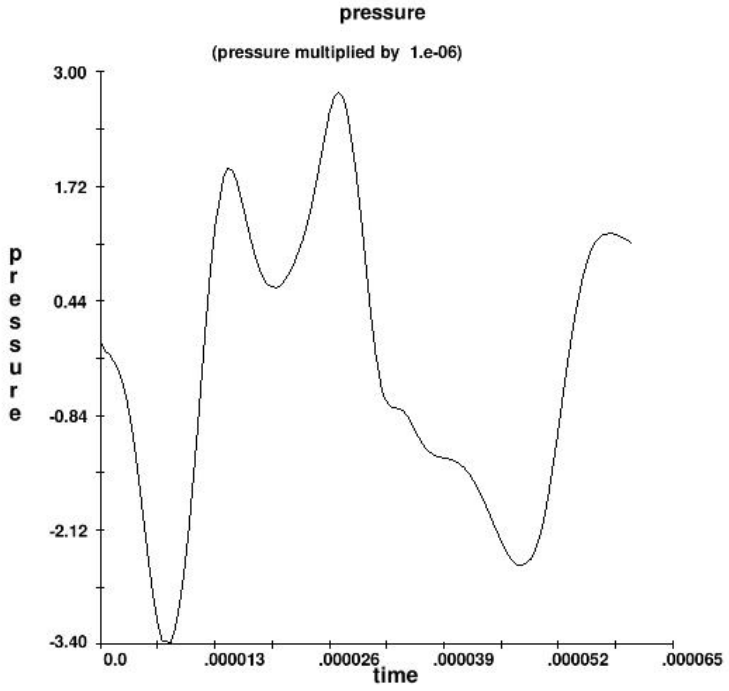

(a)

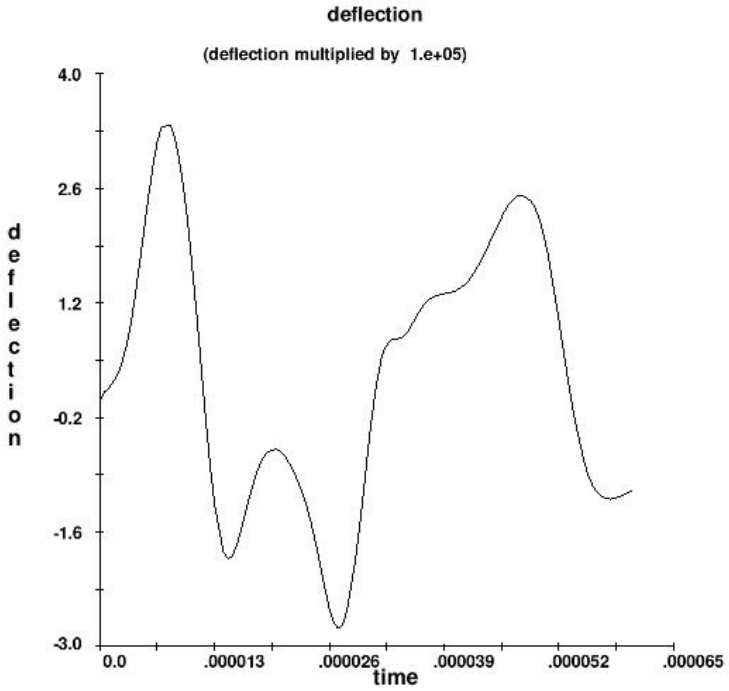

(b)

Figure 4. Pressure and deflection versus time (in s) at x=0.022 cm, y=0.0 cm, and z=0.5 cm in CGS units: (a) fluid pressure (in dyne/cm^2), (b) deflection (in cm).

5.2. Piezoelectric micro-pump

Unlike a conventional pump, a piezoelectric micro-pump uses two diffusers to control fluid flow, instead of valves. One diffuser is directed from the inlet toward the pump chamber and the other from the pump chamber toward the outlet. A clamped membrane vibrates under the action of an attached piezoelectric disk (actuator), forcing the fluid to flow back and forth through the diffusers. Due to the different resistances of the diffuser elements to flow in different directions, a net flow from the inlet to the outlet of the pump is obtained over the time of the vibration period.

Table 1. Pump parameters

Membrane material	Stainless steel
Membrane diameter	10 mm
Membrane thickness	0.15 mm
Membrane density	7850 kg/m^3
Membrane Young's modulus	19×10^{10} Pa
Piezoelectric disc diameter	8 mm
Piezoelectric disc thickness	0.25 mm
Piezoelectric disc Young's modulus	6.6×10^{10} Pa
Pump chamber diameter	10 mm
Pump chamber depth	0.2 mm
Liquid	water
Diffuser length	4.2 mm
Diffuser average diameter	0.29 mm
Diffuser minimum diameter	0.15 mm
Inlet and outlet pipe diameter	1.8 mm
Length of inlet and outlet pipes	100 mm

Figure 5 shows the schematic of the micro-pump. The actuator force generated by the piezoelectric disc is a sinusoidal function of time. The parameters of the pump are listed in Table 1 (Ullmann and Fono, 2002). Since the piezoelectric disc and the membrane are glued together, the effective Young's modulus of the membrane is estimated to be 13.0×10^{10} Pa (Ullmann and Fono, 2002). The fluid is water. Numerical simulations were carried out for a series of frequencies of the sinusoidal actuator force. The actuator force has an amplitude of 1.0 N and is uniformly distributed over the circular contact area 8 mm in diameter. Three computational mesh blocks are employed. A fine mesh block (534,600 cells) covers the volume from the inlet to the outlet of the pump, including the pump chamber, the diffusers and the inlet and outlet chambers of the pump. Two coarse mesh blocks covers the inlet and outlet pipes. The total number of mesh cells is 566,060. Static fixed-pressure boundary conditions are used at the inlet and outlet of the computational domain, with equal values of the pressure.

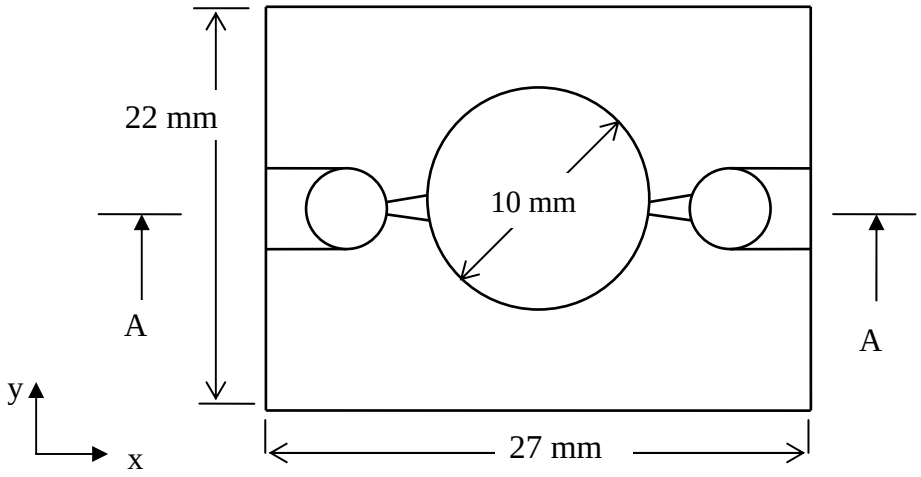

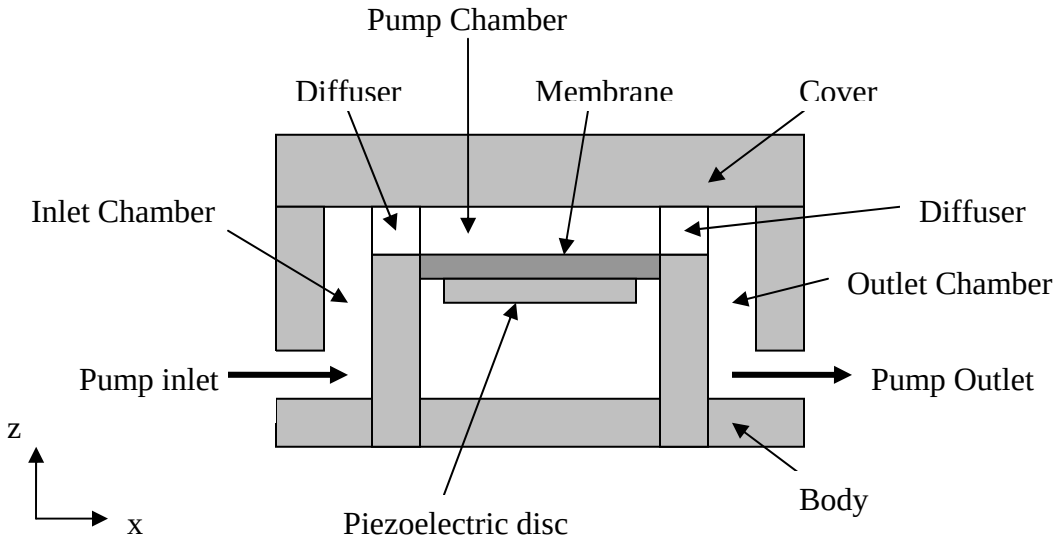

Figure 5. Schematic of the piezoelectric pump (inlet and outlet pipes are not shown).

Figure 6 shows the deflection of the membrane center versus time at 400 Hz frequency of the actuator force oscillations. It includes the effects of both the actuator force and the hydraulic pressure force. Positive deflection is in the +z direction. Figure 7 shows the distribution of deflection over the membrane's surface at two time instances, with the membrane being the circular region at the center of the figure. Figure 8 shows the 3D pressure distribution in the fluid corresponding to the deflections in Figure 7. The pressure in the chamber is high in Figure 8 (a) and low in Figure 8 (b) because fluid is in compression and expansion at these respective time instances.

Figure 9 shows the time variation of the volume flow rate through the pump at the actuator force frequency of 400 Hz. Water flows in both directions, but the time-averaged net flow rate is positive, namely, water is pumped from its inlet to outlet. Figure 10 compares the calculated and measured net volume flow rates at different frequencies of the actuator force. It is found that the agreement between the calculated and measured results is reasonably good, especially between their peak values. However, the calculated natural frequency of the pump, i.e., the frequency corresponding to the highest flow rate, is about 125 Hz larger than in the measurement. This may be due to the inaccurate pump geometry used in simulation. Some key parameters of the experimental setup in (Ullmann and Fono, 2002) are unclear, such as the exact size and shape of the diffusers and the lengths of the inlet and outlet pipes. Estimates had to be made for those parameters for the simulation. Another reason for the discrepancies may be the insufficient accuracy of the estimation of Young's modulus for the membrane-actuator assembly.

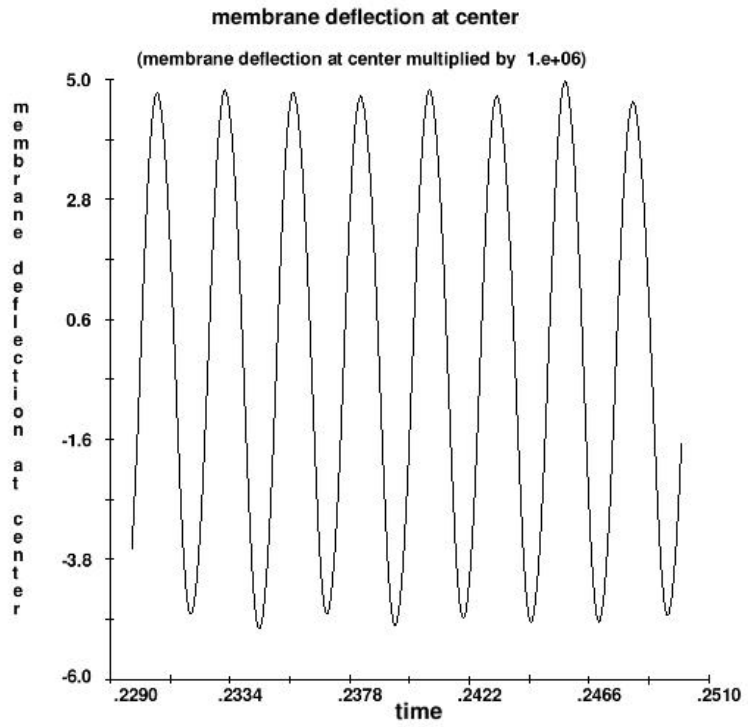

Figure 6. Deflection (units are meters) of the membrane center versus time (units are seconds) at 400 Hz vibration frequency.

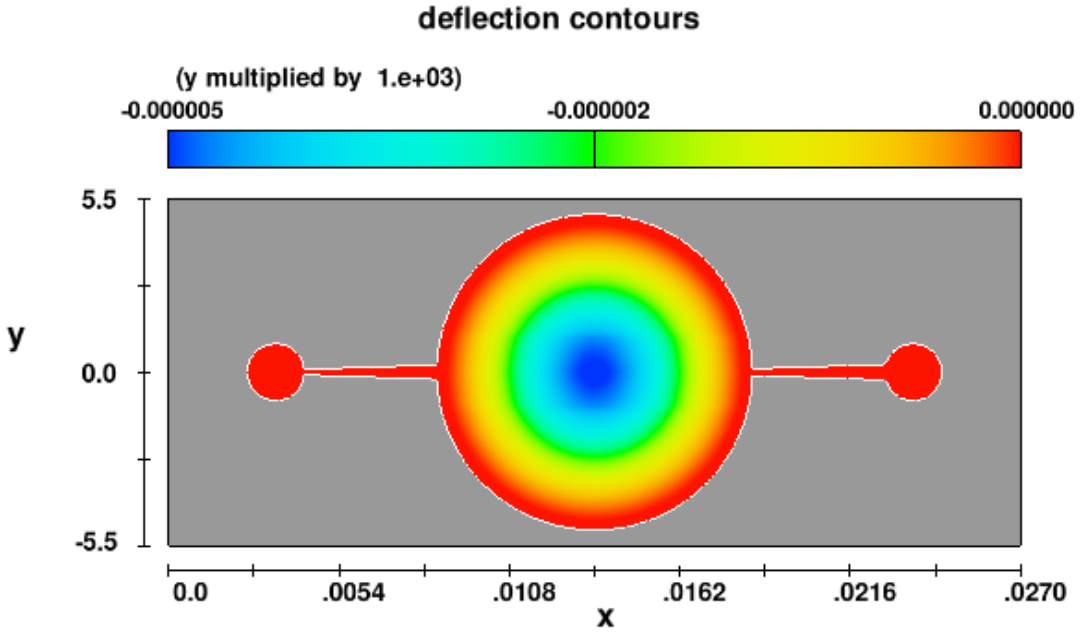

(a) t=0.312 s

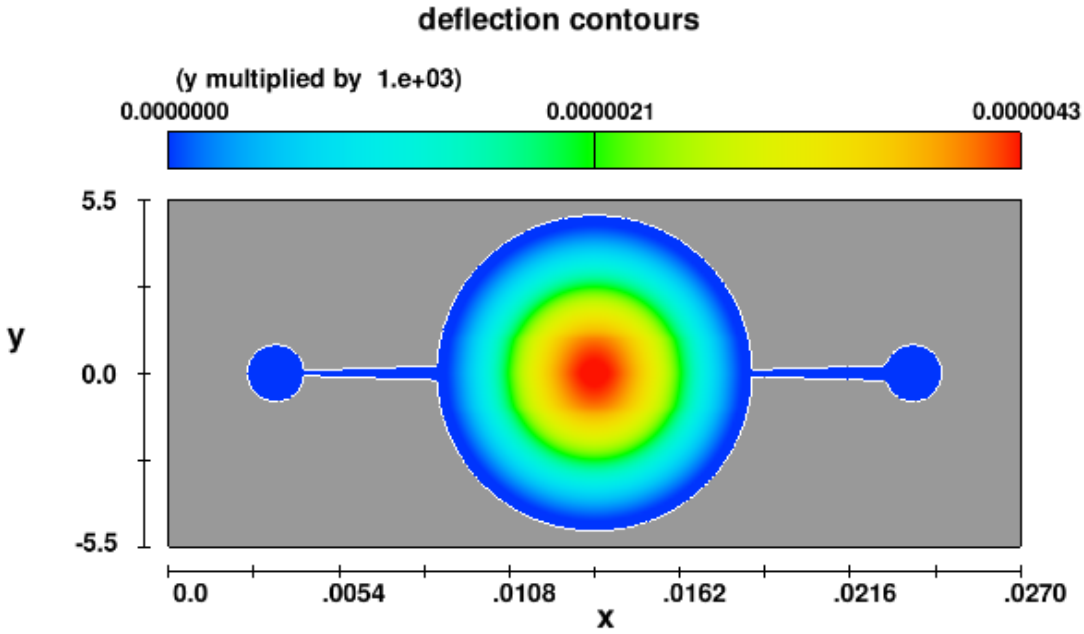

(b) t=0.316 s

Figure 7. Deflection distribution (units are meters) of the membrane at 400 Hz vibration frequency. The circular region in the center of the figure is the membrane.

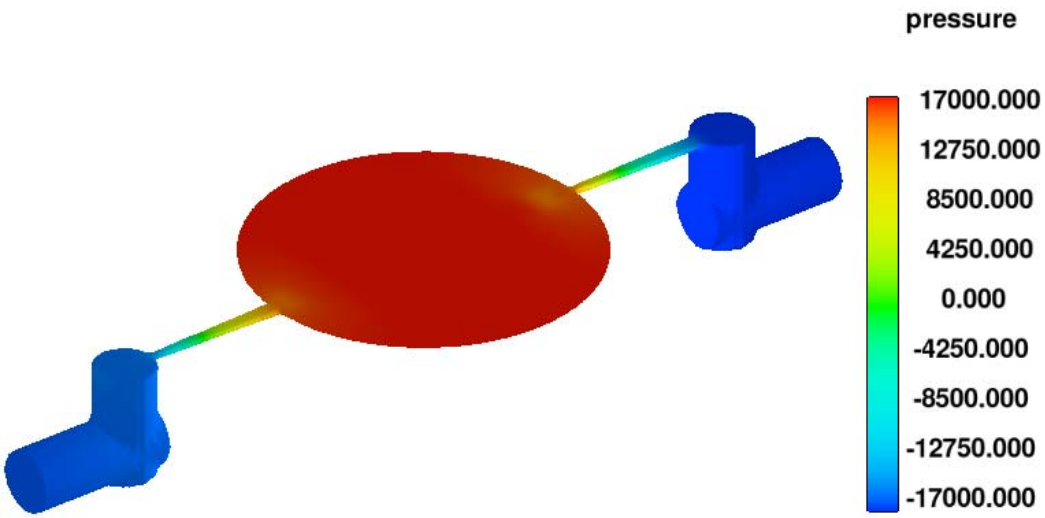

(a) t=0.312 s

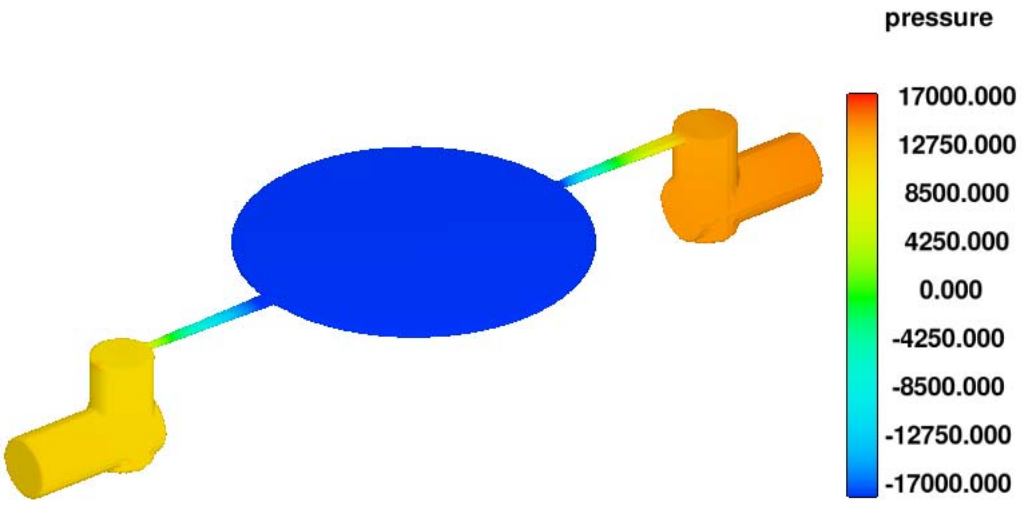

(b) t=0.316 s

Figure 8. Pressure distribution (units are Pa) at 400 Hz vibration frequency (the inlet and outlet pipes are not shown): (a) fluid is in compression near the membrane, (b) fluid is in expansion near the membrane.

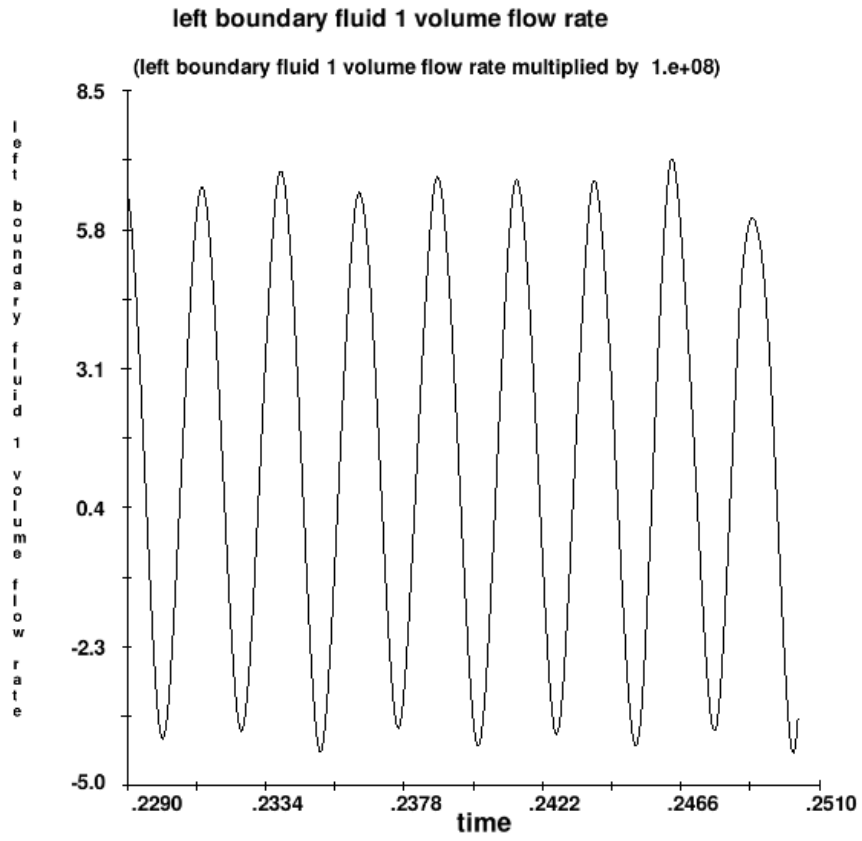

Figure 9. Volume flow rate of the pump (units are m^3/s) versus time (units are seconds).

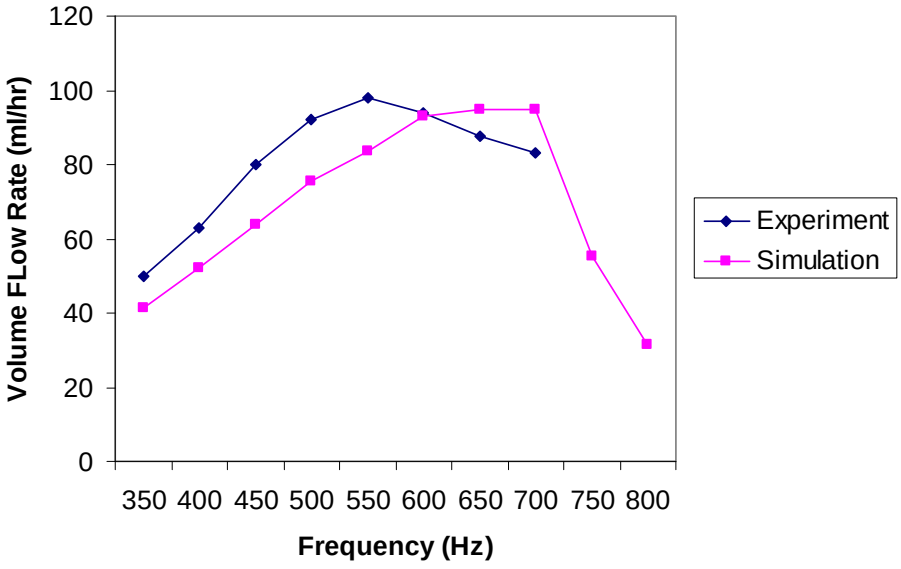

Figure 10. The net volume flow rate of the pump versus the frequency of the actuator force.

6. Conclusions

A new elastic membrane and wall deformation model, based on the small-deformation assumption, has been developed and added to ***FLOW-3D***. It can simulate deformation of an elastic membrane in response to the ambient hydraulic pressure and actuator forces. Fluid flow and membrane deformation are solved in a coupled fashion. The elastic membrane can be a rectangular or circular plate with its edge either simply supported or clamped. An actuator is assumed to be centered on the membrane and have a contact area the same shape as that of the membrane. The normal force exerted by the actuator on the membrane – the actuator force, is a user-prescribed force and can be given as a sinusoidal or a piecewise linear function of time. It can be concentrated on the membrane center or uniformly distributed over the contact area. The model also simulates elastic deformations of walls coupled with the fluid flow. An elastic wall is a solid geometry component of arbitrary shape, and its deflection at any point on the surface is in the surface normal and proportional to fluid pressure.

The model allows for multiple elastic wall and membrane components with independent properties. The model is compatible with most other models, e.g., heat transfer. For limitations of the model, the elastic membrane or wall components cannot be porous or moving. If a moving object collides with a membrane or an elastic wall, the latter is treated as a non-moving rigid object in the collision simulation.

The capabilities of the model are demonstrated by simulations of flow in a piezoelectric valveless pump and the inkjet formation for a piezo-acoustic inkjet device. Mechanisms of these devices are successfully captured. A good agreement between the computational and experimental results is obtained for the piezoelectric valveless pump case.

References

Timoshenko, S. and Woinowsky-Krieger, S., *Theory of Plates and Shells*, 2nd Edition, McGraw-Hill Inc., Auckland, 1959.

Ullmann, A. and Fono, I., *The piezoelectric valve-less pump-improved dynamical model*, Journal of Microelectromechanical Systems, Vol. 11, No. 6, 2002.

Appendix A. Analytical solutions of membrane deflection

A.1. Rectangular membrane with simply supported edge

1. Uniformly loaded

$$w = \frac{16F}{\pi^6 Dab} \sum_{m=1,3,5}^{\infty} \sum_{n=1,3,5}^{\infty} \frac{\sin\left[\frac{m\pi}{a}\left(x+\frac{a}{2}\right)\right]\sin\left[\frac{n\pi}{b}\left(x+\frac{b}{2}\right)\right]}{mn\left(\frac{m^2}{a^2}+\frac{n^2}{b^2}\right)^2} .$$

2. Centrally loaded

$$w = \frac{4F}{\pi^4 Dab} \sum_{m=1,3,5}^{\infty} \sum_{n=1,3,5}^{\infty} \frac{(-1)^{\frac{m+n}{2}-1}}{\left(\frac{m^2}{a^2}+\frac{n^2}{b^2}\right)^2} \sin\left[\frac{m\pi}{a}\left(x+\frac{a}{2}\right)\right]\sin\left[\frac{n\pi}{b}\left(x+\frac{b}{2}\right)\right] .$$

3. Partially loaded

The rectangular loaded area has the extensions a_f and b_f in x and y directions. The deflection distribution is obtained as

$$w = \frac{16F}{\pi^6 Da_f b_f} \sum_{m=1,3,5}^{\infty} \sum_{n=1,3,5}^{\infty} \frac{(-1)^{\frac{m+n}{2}-1}}{mn\left(\frac{m^2}{a^2}+\frac{n^2}{b^2}\right)^2} \sin\frac{m\pi a_f}{2a}\sin\frac{n\pi b_f}{2a} \cdot \sin\left[\frac{m\pi}{a}\left(x+\frac{a}{2}\right)\right]\sin\left[\frac{n\pi}{b}\left(x+\frac{b}{2}\right)\right]$$

A.2. Rectangular membrane with clamped edge

1. Uniformly loaded

$w = w_0 + w_1 + w_2$,

where

$$w_0 = \frac{4Fa^3}{\pi^5 bD} \sum_{m=1,3,5}^{\infty} \frac{(-1)^{\frac{m-1}{2}}}{m^5} \cos\frac{m\pi x}{a}\left(1 - \frac{\alpha_m \tanh\alpha_m + 2}{2\cosh\alpha_m}\cosh\frac{m\pi y}{a} + \frac{m\pi y}{2a\cosh\alpha_m}\sinh\frac{m\pi y}{a}\right).$$

$$w_1 = -\frac{a^2}{2\pi^2 D}\sum_{m=1,3,5}^{\infty} E_m \frac{(-1)^{\frac{m-1}{2}}}{m^2\cosh\alpha_m}\cos\frac{m\pi x}{a}\left(\frac{m\pi y}{a}\sinh\frac{m\pi y}{a} - \alpha_m \tanh\alpha_m \cosh\frac{m\pi y}{a}\right),$$

$$w_2 = -\frac{b^2}{2\pi^2 D}\sum_{m=1,3,5}^{\infty} F_m \frac{(-1)^{\frac{m-1}{2}}}{m^2\cosh\beta_m}\cos\frac{m\pi y}{b}\left(\frac{m\pi x}{b}\sinh\frac{m\pi x}{b} - \beta_m \tanh\beta_m \cosh\frac{m\pi x}{b}\right).$$

where $\alpha_m = \frac{m\pi b}{2a}$, $\beta_m = \frac{m\pi a}{2b}$, E_m and F_m are obtained by solving the equations for the boundary conditions,

$$\left(\frac{\partial w}{\partial x}\right)_{x=\pm\frac{a}{2}} = 0, \quad \left(\frac{\partial w}{\partial y}\right)_{y=\pm\frac{b}{2}} = 0,$$

namely,

$$\left(\tanh\alpha_i + \frac{\alpha_i}{\cosh^2\alpha_i}\right)E_i + \sum_{m=1,3,5}^{\infty}\frac{8i^2 a}{\pi b m^3\left(\frac{a^2}{b^2}+\frac{i^2}{m^2}\right)^2}F_m = \frac{4Fa}{\pi^3 i^3 b}\left(\frac{\alpha_i}{\cosh^2\alpha_i} - \tanh\alpha_i\right),$$

$$\left(\tanh\beta_i + \frac{\beta_i}{\cosh^2\beta_i}\right)F_i + \sum_{m=1,3,5}^{\infty}\frac{8i^2 b}{\pi a m^3\left(\frac{b^2}{a^2}+\frac{i^2}{m^2}\right)^2}E_m = \frac{4Fb}{\pi^3 i^3 a}\left(\frac{\beta_i}{\cosh^2\beta_i} - \tanh\beta_i\right),$$

where i=1,3,5,…

2. Centrally loaded

$w = w_0 + w_1 + w_2$,

where

$$w_0 = \frac{Fa^2}{2\pi^3 D}\sum_{m=1,3,5}^{\infty}\frac{1}{m^3}\cos\frac{m\pi x}{a}\cdot$$
$$\left[\left(\tanh\alpha_m - \frac{\alpha_m}{\cosh^2\alpha_m} + \frac{m\pi y}{a}\right)\cosh\frac{m\pi y}{a} - \left(1 + \frac{m\pi y}{a}\tanh\alpha_m\right)\sinh\frac{m\pi y}{a}\right]$$

$$w_1 = -\frac{a^2}{2\pi^2 D}\sum_{m=1,3,5}^{\infty} E_m \frac{(-1)^{\frac{m-1}{2}}}{m^2\cosh\alpha_m}\cos\frac{m\pi x}{a}\left(\frac{m\pi y}{a}\sinh\frac{m\pi y}{a} - \alpha_m \tanh\alpha_m \cosh\frac{m\pi y}{a}\right),$$

$$w_2 = -\frac{b^2}{2\pi^2 D}\sum_{m=1,3,5}^{\infty} F_m \frac{(-1)^{\frac{m-1}{2}}}{m^2 \cosh\beta_m}\cos\frac{m\pi y}{b}\left(\frac{m\pi x}{b}\sinh\frac{m\pi x}{b} - \beta_m \tanh\beta_m \cosh\frac{m\pi x}{b}\right),$$

where $\alpha_m = \frac{m\pi b}{2a}$, $\beta_m = \frac{m\pi a}{2b}$, E_m and F_m are obtained by solving the equations for the boundary conditions,

$$\left(\frac{\partial w}{\partial x}\right)_{x=\pm\frac{a}{2}} = 0, \quad \left(\frac{\partial w}{\partial y}\right)_{y=\pm\frac{b}{2}} = 0,$$

Namely,

$$\left(\tanh\alpha_i + \frac{\alpha_i}{\cosh^2\alpha_i}\right)E_i + \sum_{m=1,3,5}^{\infty}\frac{8i^2 a}{\pi b m^3\left(\frac{a^2}{b^2}+\frac{i^2}{m^2}\right)^2}F_m = \frac{(-1)^{\frac{i+1}{2}}F\alpha_i \tanh\alpha_i}{i\pi\cosh\alpha_i},$$

$$\left(\tanh\beta_i + \frac{\beta_i}{\cosh^2\beta_i}\right)F_i + \sum_{m=1,3,5}^{\infty}\frac{8i^2 b}{\pi a m^3\left(\frac{b^2}{a^2}+\frac{i^2}{m^2}\right)^2}E_m = \frac{(-1)^{\frac{i+1}{2}}F\beta_i \tanh\beta_i}{i\pi\cosh\beta_i},$$

where *i*=1,3,5,…

3. Partially loaded

The rectangular loaded area has extensions a_f and b_f in x and y directions. Using superposition method, the deflection distribution is obtained as

$$w = w_0 + w_1 + w_2,$$

In the loaded portion,

$$w_0 = \sum_{m=1,3,5}^{\infty}(-1)^{\frac{m-1}{2}}\left(a_m + A_m\cosh\frac{m\pi y}{a} + B_m\frac{m\pi y}{a}\sinh\frac{m\pi y}{a}\right)\cos\frac{m\pi y}{a},$$

where

$$a_m = \frac{4qa^4}{\pi^5 m^5 D}(-1)^{\frac{m-1}{2}}\sin\frac{m\pi u}{a},$$

$$A_m = -\frac{a_m}{\cosh\alpha_m}\left[\cosh(\alpha_m - 2\gamma_m) + \gamma_m\sinh(\alpha_m - 2\gamma_m) + \alpha_m\frac{\sinh 2\gamma_m}{2\cosh\alpha_m}\right],$$

$$B_m = \frac{a_m}{2\cosh\alpha_m}\cosh(\alpha_m - 2\gamma_m),$$

In the unloaded portion,

$$w_0 = \sum_{m=1,3,5}^{\infty}(-1)^{\frac{m-1}{2}}\left(A'_m\cosh\frac{m\pi y}{a} + B'_m\frac{m\pi y}{a}\sinh\frac{m\pi y}{a} + C'_m\sinh\frac{m\pi y}{a} + D'_m\frac{m\pi y}{a}\cosh\frac{m\pi y}{a}\right)\cos\frac{m\pi x}{a}$$

where

$$A'_m = A_m - a_m(\gamma_m\sinh 2\gamma_m - \cosh 2\gamma_m),$$

$$B'_m = B_m - \frac{a_m}{2}\cosh 2\gamma_m,$$

$$C'_m = a_m(\gamma_m\cosh 2\gamma_m - \sinh 2\gamma_m),$$

$$D'_m = \frac{a_m}{2}\sinh 2\gamma_m.$$

For both loaded and unloaded portions,

$$w_1 = -\frac{a^2}{2\pi^2 D}\sum_{m=1,3,5}^{\infty}E_m\frac{(-1)^{\frac{m-1}{2}}}{m^2\cosh\alpha_m}\cos\frac{m\pi x}{a}\left(\frac{m\pi y}{a}\sinh\frac{m\pi y}{a} - \alpha_m\tanh\alpha_m\cosh\frac{m\pi y}{a}\right),$$

$$w_2 = -\frac{b^2}{2\pi^2 D}\sum_{m=1,3,5}^{\infty}F_m\frac{(-1)^{\frac{m-1}{2}}}{m^2\cosh\beta_m}\cos\frac{m\pi y}{b}\left(\frac{m\pi x}{b}\sinh\frac{m\pi x}{b} - \beta_m\tanh\beta_m\cosh\frac{m\pi x}{b}\right),$$

where $\alpha_m = \frac{m\pi b}{2a}$, $\beta_m = \frac{m\pi a}{2b}$, E_m and F_m are obtained by solving the equations for the boundary conditions,

$$\left(\frac{\partial w}{\partial x}\right)_{x=\pm\frac{a}{2}} = 0, \quad \left(\frac{\partial w}{\partial y}\right)_{y=\pm\frac{b}{2}} = 0,$$

For the first equation

$$\left(\tanh\alpha_i + \frac{\alpha_i}{\cosh^2\alpha_i}\right)E_i + \sum_{m=1,3,5}^{\infty}\frac{8i^2 a}{\pi b m^3\left(\frac{a^2}{b^2} + \frac{i^2}{m^2}\right)^2}F_m,$$

$$= \frac{2\pi^2 i^2 D}{a^2}\left[\left(A_i' + B_i' + \alpha_i D_i'\right)\sinh\alpha_i + \left(C_i' + D_i' + \beta_i B_i'\right)\cosh\alpha_i\right],$$

where i=1,3,5,…

$$\alpha_i = \frac{i\pi b}{2a},$$

$$A_i = -\frac{a_i}{\cosh\alpha_i}\left[\cosh\left(\alpha_i - 2\gamma_i\right) + \gamma_i \sinh\left(\alpha_i - 2\gamma_i\right) + \alpha_i \frac{\sinh 2\gamma_i}{2\cosh\alpha_i}\right],$$

$$B_i = \frac{a_i}{2\cosh\alpha_i}\cosh\left(\alpha_i - 2\gamma_i\right),$$

$$A_i' = A_i - a_i\left(\gamma_i \sinh 2\gamma_i - \cos 2\gamma_i\right),$$

$$B_i' = B_i - \frac{a_i}{2}\cos 2\gamma_i,$$

$$C_i' = a_i\left(\gamma_i \cosh 2\gamma_i - \sinh 2\gamma_i\right),$$

$$D_i' = \frac{a_i}{2}\sinh 2\gamma_i,$$

$$a_i = \frac{4Fa^4}{\pi^5 i^5 D a_f b_f}(-1)^{\frac{i-1}{2}}\sin\frac{i\pi u}{2a}, \qquad \gamma_i = \frac{i\pi v}{4a}.$$

The second equation is similar to the first equation with E_i replaced by F_i, F_m replaced by E_m, a exchanged with b, and u exchanged with v and all the expressions for α', A_i, B_i, A'_i, B'_i, C'_i, D'_i, a_i, and γ_i. E_i, and F_i.

A.3. Circular membrane with simply supported edge

1. Uniformly loaded

$$w = \frac{F\left(a^2 - r^2\right)}{64\pi D a^2}\left(\frac{5+\nu}{1+\nu}a^2 - r^2\right),$$

where a is radius of the membrane, and r is distance from membrane's center.

2. Centrally loaded

$$w = \frac{F}{16\pi D}\left[\frac{3+\nu}{1+\nu}\left(a^2 - r^2\right) + 2r^2 \ln\frac{r}{a}\right].$$

3. Partially loaded

Assume force *F* is uniformly loaded in region $r < b$. In the unloaded portion ($a \le r \le b$),

$$w = \frac{b^2 M_b}{D\,(a^2 - b^2)}\left(-\frac{a^2 - r^2}{2(1+\nu)} + \frac{a^2}{(1-\nu)}\ln\frac{r}{a}\right) + \frac{F}{8\pi D}\left(\frac{(3+\nu)(a^2 - r^2)}{2(1+\nu)} + r^2 \ln\frac{r}{a}\right).$$

where M_b is the bending moment per unit length at $r = b$,

$$M_b = \frac{F}{16\pi a^2}(a^2 - b^2)(1-\nu)\left[1 + 2(1+\nu)\ln\frac{a}{b}\right].$$

In the loaded portion ($r < b$),

$$w = \frac{F}{64\pi b^2 D}\left(\frac{5+\nu}{1+\nu}b^2 - r^2\right)(b^2 - r^2) + \frac{M_b}{2D(1+\nu)}(b^2 - r^2) + w_b,$$

where w_b is the deflection at $r = b$ and can be obtained from the deflection expression in the unloaded region.

A.4. Circular membrane with clamped edge

1. Uniformly loaded

$$w = \frac{F}{64\pi a^2 D}\left(a^2 - r^2\right)^2.$$

2. Centrally loaded

$$w = \frac{r^2 F}{8\pi D}\ln\frac{r}{a} + \frac{F}{16\pi D}(a^2 - r^2).$$

3. Partially loaded

Assume force *F* is uniformly loaded in region $r < b$. Using the superposition method, the deflection is equal to that for a membrane with simply supported edge plus that due to the bending moment at the clamped edge. In the unloaded portion ($a \le r \le b$),

$$w = \frac{b^2 M_b}{D\,(a^2 - b^2)}\left(-\frac{a^2 - r^2}{2(1+\nu)} + \frac{a^2}{(1-\nu)}\ln\frac{r}{a}\right) + \frac{F}{8\pi D}\left(\frac{(3+\nu)(a^2 - r^2)}{2(1+\nu)} + r^2 \ln\frac{r}{a}\right)$$
$$+ \frac{M_a}{2D(1+\nu)}(a^2 - r^2)$$

where M_b is the bending moment per unit length at $r = b$,

$$M_b = \frac{F}{16\pi a^2}(a^2 - b^2)(1-\nu)\left[1 + 2(1+\nu)\ln\frac{a}{b}\right],$$

M_a is the bending moment per unit length at $r = a$,

$$M_a = \frac{2b^2 M_b}{(1-\nu)(a^2 - b^2)} - \frac{F}{4\pi} = \frac{b^2 F}{8\pi a^2}\left[1 - 2(1+\nu)\ln\frac{b}{a}\right] - \frac{F}{4\pi}.$$

In the loaded portion ($r < b$),

$$w = \frac{F}{64\pi b^2 D}(b^2 - r^2)\left[\frac{5+\nu}{1+\nu}b^2 - r^2\right] + \frac{M_b}{2D(1+\nu)}(b^2 - r^2) + w_b + \frac{M_a}{2D(1+\nu)}(a^2 - r^2),$$

where w_b is the deflection at $r = b$ for simply supported edge and can be obtained from the deflection expression in the unloaded region for simply supported edge.